VOLCANIC SPREADING AT OLYMPUS MONS: NEW MODELS, WITH IMPLICATIONS FOR MARTIAN VOLCANIC EDIFICE STRUCTURES AND THE DISTRIBUTION OF PHYLLOSIAN SEDIMENTS. P. J. McGovern[1] and J. K. Morgan[2], [1]Lunar and Planetary Institute, 3600 Bay Area Blvd., Houston TX 77058, USA (mcgovern@lpi.usra.edu), [2]Department of Earth Science, Rice University, Houston, TX 77005, USA (morganj@rice.edu),

Introduction: The 600-km-diameter Olympus Mons volcano on Mars towers some 23 km above the surrounding plains. The relatively gentle slopes of the edifice are bounded in some sectors by an escarpment (basal scarp) of height up to 10 km. Broad lobes of rough terrain (the Olympus Mons aureole deposits) partially cover the lowlands surrounding the edifice. The scarp and aureole units are most likely the results of large-scale flank failure [1-3] caused by lateral flank movement (edifice spreading) [1-5], facilitated by a basal low-friction zone (decollement) [2, 4, 5-7]. Furthermore, the presence of, and spatial variations in, a basal decollement can be inferred from topographic and tectonic asymmetries of the Olympus Mons edifice [8,9]. Decollements in terrestrial settings are often rooted in layers composed of materials with low hydraulic diffusivity, such as clays [10]. Phyllosilicate (clay) minerals have been detected by recent missions to Mars [11-12], and are inferred to have been widely emplaced during an epoch, termed the "Phyllosian", that overlaps (but ends before) the Noachian [12].

Here we present new numerical models of edifice spreading and flank failure to improve constraints on the conditions (including spatial variations in basal friction) that produce observed edifice structures and asymmetries of Olympus Mons. We then discuss the implications of these models for the distribution of phyllosilicate sediments and the structures of large volcanoes on Mars.

Structure of Olympus Mons: The edifice of Olympus Mons exhibits several characteristics of volcanic spreading, including concave-upward lower flank topography, faulting (both extensional and compressional), and a large basal scarp, sectors of which constitute the headscarps of giant landslides (the Olympus Mons aureoles) [8,9]. However, these features are distributed asymmetrically. The northwest (NW) flank extends almost 80 km further from the central caldera complex than the southeast (SE) flank, and mean flank slopes are a degree or two lower for the NW flank vs. the SE. [8,9]. The NW flank exhibits several distal sub-radial normal faults, whereas the SE flank contains a wide zone of proximal compressional terraces [13] and evidence for distal upthrusting and scraping of crustal blocks.

Models: Following earlier modeling efforts [9, 14], we produce two-dimensional numerical simulations using the Distinct Element Method (DEM). The method resolves contact forces acting on discrete particles, and solves Newton's equations of motion for each particle to maintain quasi-static equilibrium of the assemblages. Growth of the volcanic edifice is simulated by "raining" frictional particles upon a planar substrate. Once each increment of particles has settled, particle positions, contacts, and forces are recorded for processing. The radius and friction coefficient of the basal layer of particles set the characteristic basal friction μ_b of the volcano/substrate interface. Various configurations of lateral variations in basal friction are modeled; in most cases, a low-friction central region is superposed, to account for the effects of a fluid-filled magma chamber beneath the summit.

The simplest models, with constant-friction flanks, fail to generate concave-upward slopes or flank asymmetry. Deformation is concentrated near the center of the load; far from this zone, the flanks appear to spread outward as uniform wedges with little internal deformation. In contrast, models with laterally varying basal friction produce greater variations in flank morphology and deformation. Models with basal friction increasing to the right (Figs. 1, 2) produce strongly concave flank topography on the low-friction side but convex on the high-friction side. The highest summit topography tends to be on the high-friction side. Deformation is also asymmetric: narrow bands of extensional deformation resembling graben are evident on the low-friction flank (Figure 2, left side of middle and bottom panels), but the high-friction flank moves as a nearly rigid block, generally experiencing compression (blue shading on right side of Figure 2, middle panel). The low-friction flank experiences a decreasing amount of support as it expands outward, leading to a "cascade" of motion as the proximal flank must deform to accommodate the greater tendency of distal material to move. Models with friction decreasing outward from the center (except for the low friction central patch) also produce extensional faulting and prominent concave-upward flanks (on both sides). Superposed with a regional slope or a broader ramp in basal friction (as in Fig. 1), such models yield asymmetric flank slopes and widths, and diminished fault-like deformation on the upslope side in the final load increments.

Discussion: Olympus Mons is located on the margins of the Tharsis rise, east of the smooth lowland plains of Amazonis. The modeling presented above indicates that the structural features of the Olympus Mons edifice, scarp, and aureole described are best explained by a gradient in basal friction beneath the edifice, increasing toward the southwest (e.g, with proximity to the Tharsis rise). Such a gradient is consistent with a decrease in sediment thickness with increasing elevation, as would be expected if sediments are transported from sources (highlands) to sinks (lowland basins). Sediment creation would be most vigorous during the Noachian (essentially, Phyllosian), when climate conditions were most conductive to fluvial erosion. The recent spectroscopic observations [11-12] indicate that formation of phyllosilicates would be chemically favored during this epoch; thus, a large fraction of such sediments could be clays.

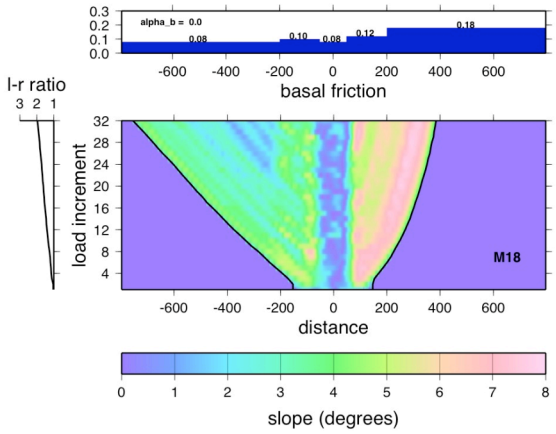

Figure 1. Central Plot: color map of flank slope as a function of horizontal distance from center (x-axis) and load increment (or time; y-axis) for a DEM model of volcanic spreading. The edge of the edifice at each timestep is traced by the black lines. The top set of axes shows the basal friction on the y-axis vs. the same distance axis. The rightmost axis shows the ratio of flank lengths (left over right).

If Phyllosian/Noachian sediments were distributed preferentially in lowlands, then volcanoes at low basal elevations elsewhere on mars are the most likely to have basal detachments. Large volcanoes in the lowlands are generally lacking, but Apollinaris Patera (AP), like Olympus Mons, is located at the highland-lowland transition. AP has several features consistent with Olympus Mons-style basal spreading: concave-up flank slopes and a partial basal escarpment with distributed broken-up terrain beneath and surrounding it (a potential aureole analog). AP is near the mouth of Ma'adim Valles, which may have yielded a large supply of sediments from the highlands to the base of AP. Conversely, the bases of the Tharsis Montes are at very high elevations on the Tharsis Rise, and therefore unlikely to exhibit significant thicknesses of phyllosilicate sediment. This inference is consistent with the absence of spreading-related structures (scarps, aureoles); the abundant extensional features on these edifices are likely to be related to intrusion [e.g., 15, 16] rather than spreading. Similarly, highland paterae and shields (Tyrrhena, Hadriaca, Syrtis Major, etc.) are based at relatively high elevations, rendering them unlikely locations for large accumulations of sediment. The older ages of these structures relative to the Tharsis volcanoes also suggests that construction of edifices may have started well before the end of phyllosilicate production, further reducing the potential for basal sediments and the resulting enhancement of volcanic spreading.

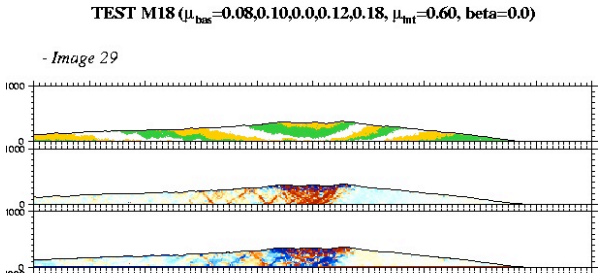

Figure 2. Stratigraphy and deformation in the volcanic pile, for the same model of volcanic spreading as in Figure 1, and for distances within 500 km of the center. Top panel: Color-coded stratigraphy denoted by green, gold, and white layers. Each color layer constitutes 300-element load increments. Middle panel: Lagrangian horizontal normal strain. Red denotes extension, blue contraction. Lower panel: Second invariant of the deviatoric strain tensor. Strain magnitude is denoted by color intensity, with red colors indicating rightward-directed motion and blue leftward-directed motion. No vertical exaggeration.

References: [1] R. M. Lopes et al., *JGR, 87*, 9917, 1982; [2] P. J. McGovern and S. C. Solomon, *JGR, 98*, 23,553, 1993; [3] P. J. McGovern et al., *JGR, 107*, doi10.1029/ 2004JE002258, 2004; [4] A. Borgia et al., *JGR, 95*, 14,357, 1990; [5] P. W. Francis and G. Wadge *JGR, 88*, 9333, 1983; [6] K. L. Tanaka, *Icarus, 62*, 191, 1985; [7] S. A. Harris, *JGR, 82*, 3099, 1977; [8] P. J. McGovern et al., *LPS, 37*, 2329, 2006; [9] P. J. McGovern et al., *7th Int. Conf. Mars*, 3397, 2007; [10] R. M. Iverson, JVGR, 66, 295, 1995; [11] F. Poulet et al., *Nature, 438*, 623, 2005; [12] J.-P. Bibring et al., *Science, 312*, 400, 2006; [13] P. J. Thomas et al., *JGR, 95*, 14,345, 1990; [14] J. K. Morgan and P. J. McGovern, JGR, doi10.1029/2004JB003252, 2005; [15] L. G. J. Montesi, *GSA Spec. Pap. 352*, 165, 2001;[16] P. J. McGovern et al., *JGR, 106*, 23,769. 2001.